Classical simulation of atomic beam focusing and deposition for atom lithography

Xianzhong Chen (陈献忠), Hanmin Yao (姚汉民), and Xunan Chen (陈旭南)

State Key Laboratory of Optical Technologies for Microfabrication,
Institute of Optics and Electronics, Chinese Academy of Sciences, Chengdu 610209

Received December 23, 2003

We start from the intensity distribution of a standing wave (SW) laser field and deduce the classical equation of atomic motion. The image distortion is analyzed using transfer function approach. Atomic flux density distribution as a function of propagation distance is calculated based on Monte-Carlo scheme and trajectory tracing method. Simulation results have shown that source imperfection, especially beam spread, plays an important role in broadening the feature width, and the focus depth of atom lens for real atomic source is longer than that for perfect source. The ideal focal plane can be easily determined by the variation of atomic density at the minimal potential of the laser field as a function of traveling distance.

OCIS codes: 020.7010, 140.3320.

As a new technology, atom lithography enables us to write directly nanometer scale structures onto a substrate in a parallel process. In this technique, the focusing of an atomic beam to be deposited is achieved with a standing wave (SW) laser field that serves as an array of parallel atom lens. By now, this technique has been applied to some atoms including sodium[1], chromium[2−4], aluminum[5], and cesium[6]. Atom lens is based on the fundamental interaction process between atoms and photons. To account for all properties of such an atom-optical component, a fully quantum treatment is necessary. We do not follow this rigorous way here. Instead, we work in the classical method. On a more practical level, the classical calculations are less expensive in terms of computation time[7]. Researchers are very interested in atom lithography with chromium atoms because chromium is a particularly useful candidate. First, chromium has very good sticking properties on a variety of substances. Second, it is chemically stable in air, and being a standard mask substance, it is suitable for further lithography processes. Furthermore, lack of hyperfine structure in the desired atomic transition allows a particularly efficient exploitation of the optical dipole force. In this paper, we take chromium as an example to analyze laser focused atomic deposition in SW field. A thorough understanding of laser focusing process is the first step when considering applications of laser-focused deposition to quantitative surface science and nanostructure research. The influences of atomic source on atom focusing, the focus depth of the atom lens, and the determination of the ideal focal plane for atom lens are analyzed and discussed.

One period of a laser SW that is detuned far enough from the atomic resonance can be considered to form an atom lens. The light intensity distribution of SW laser field is

$$I(x,z) = I_{\max}\mathrm{e}^{-2z^2/w_0^2}\sin^2(kx), \tag{1}$$

where $I_{\max}$, w_0, and k are the maximal light intensity, $1/\mathrm{e}^2$ radius at the beam waist, and the wave vector, respectively. The SW has a fast variation along Ox with a period of half an optical wavelength, while it has a slower variation along Oz given by a Gaussian function.

If the longitudinal velocity of the atom v_z is large enough, the motion of the atom along Oz may be treated classically. Furthermore, the light force along Oz is negligible as compared with that along Ox. The laser intensity drops to 1% of the peak value at $\pm 1.5w_0$ about the Gaussian beam center, so we will take $3w_0$ as the longitudinal interaction length. From these discussions it follows that $I(x,z)$ may be replaced by the temporal profile

$$I(x,t) = I_{\max}\exp[-2\frac{(v_z t - 1.5w_0)^2}{w^2}]\sin^2(kx). \tag{2}$$

If spontaneous emissions take place and the system reaches a steady state, the potential takes the form[8]

$$U(x,t) = \frac{\hbar\Delta}{2}\ln(1+s), \tag{3}$$

where $s = 2\Omega^2/(4\Delta^2+\Gamma^2)$ is the saturation parameter, Γ is the spontaneous emission rate. Rabi frequency can be calculated from the formula $\Omega = \Gamma[I(x,t)/(2I_\mathrm{s})]^{1/2}$, where I_s is the saturation intensity.

The force acting on a two-level atom can be derived from Eqs. (2) and (3)

$$\begin{aligned} F(x,t) &= -\frac{\partial U(x,t)}{\partial x} \\ &= -\frac{a\hbar\Delta}{2}\frac{kI_{\max}\exp[-2\frac{(v_z t-1.5w_0)^2}{w_0^2}]\sin(2kx)}{(a+4)I_\mathrm{s} + aI_{\max}\exp[-2\frac{(v_z t-1.5w_0)^2}{w_0^2}]\sin^2(kx)}, \end{aligned} \tag{4}$$

where $a = \Gamma^2/\Delta^2$. If we want to describe the trajectory of moving atom, we need to solve the classical equation of motion

$$m\frac{\mathrm{d}^2x}{\mathrm{d}^2t} = F(x,t). \tag{5}$$

We start the calculation with $\lambda = 425.6$ nm, $\Gamma = 2\pi\times 5.0$ MHz, $I_\mathrm{s} = 8.5$ mW/cm^2, $\Delta = 50\Gamma$, $I_{\max} = 2.0\times 10^5$ W/m^2, $T = 1800$ K, and $w_0 = 200$ μm, some parameters are taken from Ref. [4]. Throughout the calculation, collisions among atoms are ignored.

The classical atomic trajectory is calculated employing an adaptive step size, fourth-order Adams-Moulton type algorithm. Only one period of the SW is taken into account because the assumed focusing geometry ensures an intrinsic periodicity (periodic boundary conditions). For real atom source, the longitudinal velocities obey Maxwell-Boltzmann statistics, and the initial transverse velocities are assumed to exhibit a Gaussian spread[4].

In order to gain insight into the image distortion, the transfer function approach is used to describe the relation between the initial position X_i of an atom and its final position X_f in the focal plane. In Fig. 1(a), the zero slope of $X_f(x)$ indicates the focal spot with feature size near zero. But atoms entering far from the nodes are defocused, which is termed as spherical aberration. We also use the transfer function approach to analyze the influences of velocity spread and beam spread on atom focusing. Velocity spread bends X_f in the focusing region away from the horizontal slope corresponding to infinitely sharp focusing (Fig. 1(b)), and beam spread causes X_f to be shifted (see Fig. 1(c)) from the ideal case where the atomic beam is perpendicular to the light beam. Diffusive processes such as spontaneous emission and surface migration, which are omitted here, also limit the feature width.

The atomic flux density distribution at a final longitudinal position Z can be determined by calculating a histogram of final transverse positions X at a grid. We traced 100,000 trajectories with a uniform distribution of x positions, a Gaussian distribution of transversal velocities and a Maxwell-Boltzmann distribution of longitudinal velocities, and the atomic flux density distribution as a function of propagation distance Z is shown in Fig. 2. Beam spread plays a crucial role in determining the feature width, so the preparation of a

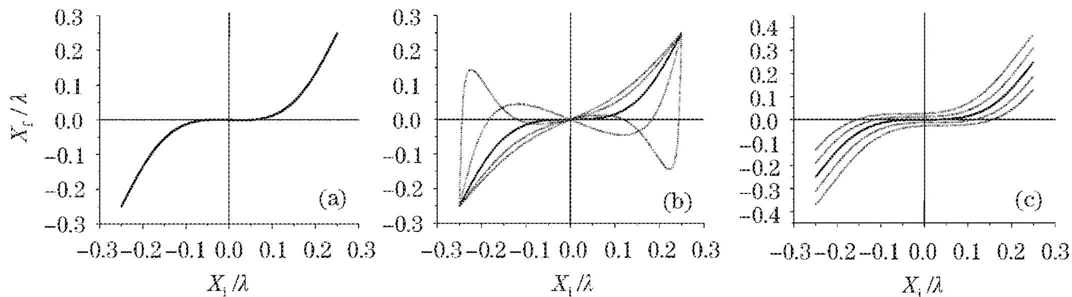

Fig. 1. The atomic coordinate at the focal plane X_f versus initial coordinate X_i, the solid lines stand for well-collimated atoms with v_z = 926 m/s and the dotted lines for atoms with other parameters. (a) An ideal atomic beam, (b) a perfectly collimated atomic beam with different longitudinal velocities, (c) a monoenergetic atomic beam with different transversal velocities.

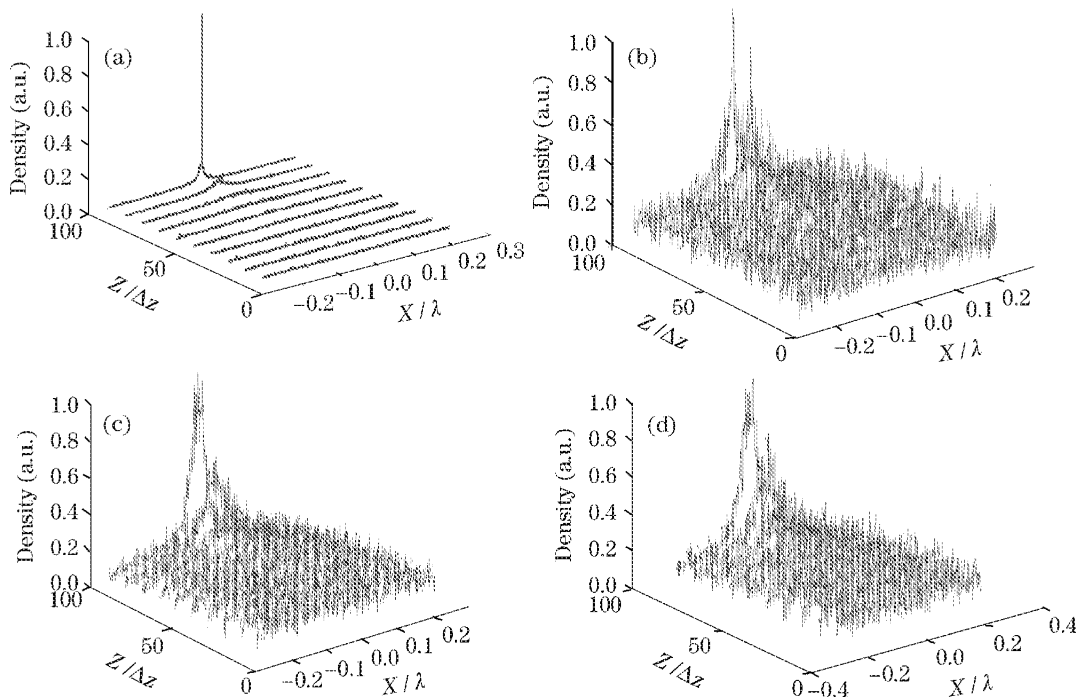

Fig. 2. Atomic flux density distribution as a function of propagation distance Z. Δz = 3 μm. (a) An ideal atomic beam, (b) a thermal, perfectly collimated atomic beam with longitudinal velocities distributed according to the Maxwell-Boltzmann distribution at a source temperature of 1800 K, (c) a monoenergetic atomic beam with an effective transversal temperature of 50 μK, and (d) a thermal atomic beam with a source temperature of 1800 K and an effective transversal temperature of 50 μK.

well-collimated and transversely cooled atomic beam is essential to minimize the severely disadvantageous effects. The influence of atom source on the focus depth of the atom lens can also be analyzed from Fig. 2. The focus depth of atom lens for real atom source (see Fig. 2(d)) is longer than that for perfect source (see Fig. 2(a)), which indicates that the substrate for ideal source must be positioned more strictly than that for real source.

Figure 3(a) is the variation of atomic flux density as a function of longitudinal traveling distance at the minimal optical potential, and the ideal focal plane coincides with the position where the atomic flux density is maximal. We can obtain nanostructure with good quality if a substrate is positioned here. Figure 3(b) is the atomic flux density distribution at the optimal focal plane, and the full width at half maximum (FWHM) of the feature observed in Fig. 3(b) is about 28.5 nm.

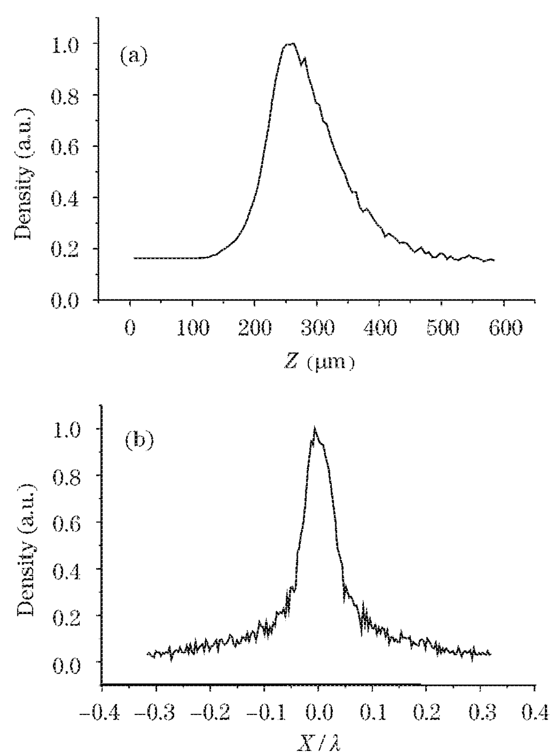

Fig. 3. (a) Variation of the atomic flux density at minimal potentials as a function of propagation distance Z, (b) atomic density distribution at the optimal focal plane in accordance with (a).

In summary, we deduced the equation of atomic motion to describe the behavior of a chromium atomic beam traveling through the SW laser field. The influences of source imperfection such as beam spread and velocity spread on the image distortion are analyzed using transfer function approach. We also calculated atomic flux density distribution during its propagation in the laser field using Monte-Carlo scheme and trajectory tracing method. Results have shown that beam spread dominates the feature width, and the position of the substrate for real atomic source is not as strict as that for perfect source. This is helpful for a good understanding of the laser focusing process. The ideal focal plane can be easily determined by the variation of atomic density at the minimal optical potential of the SW laser field as a function of propagation distance.

This work was supported by the Innovation Foundation of the Chinese Academy of Sciences under Grant No. A2K0009. X. Chen's e-mail is ioechenxiz@hotmail.com.

References

1. G. Timp, R. E. Behringer, D. M. Tennant, J. E. Cunningham, M. Prentiss, and K. K. Berggren, Phys. Rev. Lett. **69**, 1636 (1992).
2. J. J. McClelland, R. E. Scholten, E. C. Palm, and R. J. Celotta, Science **162**, 877 (1993).
3. W. R. Anderson, C. C. Bradley, J. J. McClelland, and R. J. Celotta, Phys. Rev. A **59**, 2476 (1999).
4. J. J. McClelland, J. Opt. Soc. Am. B **12**, 1761 (1995).
5. R. W. McGowan, D. M. Giltner, and S. A. Lee, Opt. Lett. **20**, 2535 (1995)
6. F. Lison, D. Haubrich, P. Schuh, and D. Meschede, Appl. Phys. B **65**, 419 (1997)
7. M. K. Olsen, T. Wong, S. M. Tan, and D. F. Walls, Phys. Rev. A **59**, 3358 (1996).
8. J. Dalibard and C. Cohen-Tannoudji, J. Opt. Soc. Am. B **2**, 1707 (1985).